Published in final edited form as:
Atmos Environ. 2009 April ; 43(12): 2018–2030. doi:10.1016/j.atmosenv.2009.01.003.

$PM_{2.5}$ Characterization for Time Series Studies: Organic Molecular Marker Speciation Methods and Observations from Daily Measurements in Denver

Steven J. Dutton[a], **Daniel E. Williams**[a], **Jessica K. Garcia**[b], **Sverre Vedal**[c], and **Michael P. Hannigan**[d]

[a] Department of Civil, Environmental and Architectural Engineering, College of Engineering and Applied Science, University of Colorado, Boulder, CO 80309, USA

[b] Department of Civil and Environmental Engineering, California Polytechnic State University, San Luis Obispo, CA 93407, USA

[c] Department of Environmental and Occupational Health Sciences, School of Public Health and Community Medicine, University of Washington, Seattle, WA 98105, USA

[d] Department of Mechanical Engineering, College of Engineering and Applied Science, University of Colorado, Boulder, CO 80309, USA

Abstract

Particulate matter less than 2.5 microns in diameter ($PM_{2.5}$) has been shown to have a wide range of adverse health effects and consequently is regulated in accordance with the US-EPA's National Ambient Air Quality Standards. $PM_{2.5}$ originates from multiple primary sources and is also formed through secondary processes in the atmosphere. It is plausible that some sources form $PM_{2.5}$ that is more toxic than $PM_{2.5}$ from other sources. Identifying the responsible sources could provide insight into the biological mechanisms causing the observed health effects and provide a more efficient approach to regulation. This is the goal of the Denver Aerosol Sources and Health (DASH) study, a multi-year $PM_{2.5}$ source apportionment and health study.

The first step in apportioning the $PM_{2.5}$ to different sources is to determine the chemical make-up of the $PM_{2.5}$. This paper presents the methodology used during the DASH study for organic speciation of $PM_{2.5}$. Specifically, methods are covered for solvent extraction of non-polar and semi-polar organic molecular markers using gas chromatography-mass spectrometry (GC-MS). Vast reductions in detection limits were obtained through the use of a programmable temperature vaporization (PTV) inlet along with other method improvements. Results are presented for the first 1.5 years of the DASH study revealing seasonal and source-related patterns in the molecular markers and their long-term correlation structure. Preliminary analysis suggests that point sources are not a significant contributor to the organic molecular markers measured at our receptor site. Several motor vehicle emission markers help identify a gasoline/diesel split in the ambient data. Findings show both similarities and differences when compared with other cities where similar measurements and assessments have been made.

Keywords

particulate matter; $PM_{2.5}$; chemical speciation; organic carbon; molecular markers

1. INTRODUCTION

Particulate matter in the atmosphere has been linked with a wide range of adverse impacts on human health (HEI, 2001, 2002; Lippmann et al., 2003). Determining the origin of these particles is critical for developing efficient and effective control strategies to help mitigate these health effects (Grahame and Schlesinger, 2007; Schwarze et al., 2006). Fine particles with aerodynamic diameters less than 2.5 μm in diameter ($PM_{2.5}$) are of particular interest in health studies due partly to their chemical composition and deposition characteristics. $PM_{2.5}$ originates from both natural and anthropogenic sources which can either directly emit particles or emit precursor gasses which subsequently form particles in the atmosphere as products of oxidation reactions. The complicated origin of $PM_{2.5}$ makes identifying the specific sources most responsible for the observed health effects a challenging task and the subject of ongoing research.

In receptor modeling, the first step in determining the origin of $PM_{2.5}$ is to chemically or physically characterize the particles observed at a receptor site. Commonly characterized components of $PM_{2.5}$ include mass, inorganic ions, total carbon and trace metals. In recent years, gas chromatography-mass spectrometry (GC-MS) analysis for organic molecular marker compounds has become a more popular option for $PM_{2.5}$ speciation (e.g., Robinson et al., 2006b; Sheesley et al., 2007; Zheng et al., 2002). Although this method has been used for several decades (e.g., Cautreels and Van Cauwenberghe, 1976), recent advancements in organic extraction procedures, analytical instrumentation and available source profiles have made it a more attractive alternative for $PM_{2.5}$ characterization and source apportionment.

Organic molecular markers are individually quantifiable organic compounds emitted by a specific source or class of sources. Some common molecular marker compound classes include alkanes, cycloalkanes, polycyclic aromatic hydrocarbons (PAHs), steranes, fatty acids, sterols and methoxyphenols. Ideally, each molecular marker would originate from one unique source type. In reality, however, they can originate from multiple source types each with their own time-dependent source contribution. Much work has been done to characterize the unique molecular marker emissions from a wide range of anthropogenic and natural sources (e.g., motor vehicles, biomass combustion, food cooking). Substantially less work, however, has been done on monitoring the daily variability of molecular markers in the ambient air. Cost, analysis time constraints and prohibitively high detection limits have restricted the scope of most previous studies. Recent work by Sheesley et al. (2007) provided the first look at a year long time series of molecular marker measurements in St. Louis. Wittig et al. (2004) present a similar data set arising from the Pittsburgh Air Quality Study, combining periods of daily and every sixth day sampling for organic molecular markers.

This paper will present the longest and most complete daily time series of organic molecular marker measurements to date spanning the first 1.5 years of the Denver Aerosol Sources and Health (DASH) study. The DASH study is a multi-year time series health effects study based in Denver, CO, with the goal of identifying associations between adverse health outcomes and $PM_{2.5}$ sources (Vedal et al., 2008). The chemical speciation focus of the DASH study has been on organic molecular markers, though mass, inorganic ions and metals have been characterized as well (Dutton et al., 2008). This paper describes the measurement methods and uncertainty estimation techniques used in quantifying non-polar and semi-polar organic molecular markers collected at the DASH receptor site in Denver. Seasonal trends and correlations among the

molecular markers observed during the first year and a half of daily measurements are also presented. Finally, results from a preliminary investigation into the influence of point sources and an indication of a gasoline/diesel split are presented together with comparison to results from other studies.

2. METHODS

2.1 $PM_{2.5}$ Sampling Protocol

The DASH study receptor site is located on the rooftop of a two story building 5.3 km east of downtown Denver. This site was chosen for its location within a residential neighborhood distant from any major industrial or point sources. A more detailed description of the site is included in Vedal et al. (2008). Sample collection started on July 1, 2002 and organic molecular marker quantification has been completed on 541 daily samples, running through December 31, 2003. In addition, 77 weekly field blanks were collected and analyzed in parallel with the other samples during this period.

$PM_{2.5}$ filter samples were collected daily from midnight to midnight with sampling equipment that has been used extensively in air quality measurement campaigns in the past (Bae et al., 2006; Jaeckels et al., 2007; Scheesley et al., 2007). A complete description of the sampling setup along with results from the bulk speciation (mass, inorganic ions, elemental carbon and total organic carbon) is available in Dutton et al. (2008). This paper focuses on the organic molecular marker analyses performed on 90 mm diameter quartz fiber filters (Pall Gelman Tissuequartz™). Strict adherence to filter collection, handling and transport methodology has been followed throughout the study to minimize organic contamination. The quartz filters were wrapped in clean aluminum foil and pre-baked in an oven at 500 ºC before being placed in pre-baked glass petri dishes for transport and pre-baked glass jars for storage. All filter handling was done with clean, solvent rinsed metal forceps. Filters were collected from the samplers within 72 hours of sampling, transported in coolers with ice packs and stored in a freezer at −25 °C prior to analysis.

2.2 Filter Extraction

Established methods for organic solvent extraction were used to extract the compounds of interest from the quartz filters for subsequent analysis (Mazurek et al., 1987; Rogge et al., 1991; Schauer et al., 1999). Prior to extraction, each filter was spiked with 25 μl of an internal standard mixture containing known concentrations of isotopically labeled compounds not present in the atmosphere. By selecting internal standards of similar structure to the molecular markers being quantified, we were able to account for variability in recovery during the extraction process (discussed further below). Table S1 in the supporting documents contains a list of the internal standard compounds utilized for this study. The internal standards were synthesized by the Wisconsin State Laboratory of Hygiene (WSLH) and have been used for organic molecular marker tracer quantification in the past (e.g., Sheesley et al., 2007).

Reagent grade methylene chloride (Fisher Scientific #D151-4, Pittsburgh, PA) was used to extract the organic compounds of interest from the quartz filters. All glassware used in the extraction process was cleaned with soap and water, rinsed in deionized water, isopropyl alcohol and hexane, baked at 500 ºC for 8 hours and given a final rinse with methylene chloride (DCM) immediately prior to use. The previously spiked filters were extracted twice by sonication in DCM for 15 minutes each, providing a total combined extract volume of 40 mL per filter. The extracts were then passed through a pre-baked glass fiber filter (Pall Gelman Type A/E) to remove any solid material and concentrated under a gentle stream of ultra high purity nitrogen to a final volume of 150 μl.

2.3 Gas Chromatography/Mass Spectrometry Analysis

The extracts were analyzed by gas chromatography-mass spectrometry (GC-MS) using an Agilent Technologies 6890N gas chromatograph (GC) attached to an Agilent 5975 Inert Mass Selective Detector (MS). The GC was equipped with a 30 meter low-bleed non-polar J&W Scientific HP-5ms capillary column with a 0.25 mm diameter bore coated in 5% phenylmethylpolysiloxane (Agilent #19091S-433). Vast improvements to the organic compound detection limits were obtained by high-volume injection using a programmable temperature vaporization (PTV) inlet (Wylie, 1997). An Agilent 7683B auto-injector equipped with a 100 μl needle (Agilent #5181-3384) was used to inject 50 μl of each sample (1/3 of the final 150 μl extract volume) onto the PTV Multi Baffle liner (Agilent #5183-2037). The PTV method allows for much larger injections than traditional GC-MS analysis, thereby vastly improving detection limits of trace level organic compounds (Crimmins and Baker, 2006). Figure S1 in the supplemental information shows the temperature and flow rate program used for the PTV and GC. A ramp rate of 30 ºC/min on the GC oven minimized the overall run time while providing adequate peak separation. A final oven temperature of 325 ºC was held for ten minutes to allow for less volatile compounds to travel through the GC column. The PTV liner was replaced and 1 m was cut from the inlet end of the GC column between every sequence (25–30 runs) to improve the quality of the chromatograms. The PTV was disassembled and cleaned with solvent, and the column was replaced when the ion chromatograms for the standards began to show signs of peak deterioration or when the column reached a minimum length of 20 m.

The MS was equipped with an inert electron ionization source and was operated in full scan mode to allow for complete spectral identification of the target compounds. Mass to charge ratios (m/z) from 50 to 500 were analyzed with unit resolution. The MS was tuned at m/z = 69, 219, and 502 prior to every sequence using perfluorotributylamine (PFTBA) as a reference standard.

2.4 Compound Quantification

Seventy-one non-polar and semi-polar organic molecular marker compounds were quantified for each sample (see Table 1 for a complete list of compounds). They included alkanes, cycloalkanes, polycyclic aromatic hydrocarbons (PAHs), methyl substituted PAHs (methyl-PAHs), oxygenated PAHs (oxy-PAHs), steranes, fatty acids, sterols and methoxyphenols. These compounds serve as markers for various emission sources (Schauer et al., 1996). The more polar organic molecular markers (e.g., levoglucosan) were not quantified in the current study since they require an extra derivatization step to be accurately quantified by GC-MS. Between one third and two thirds of each extract has been retained in cold storage for future analysis of more polar compounds with derivatization.

The samples were run on the GC-MS in sequences incorporating 14 samples and 2 field blanks. Each sequence also included six solvent blanks for quality control and five dilutions of known concentration quantification standards. The quantification standards were obtained from WSLH and contain most of the organic marker compounds of interest. The footnote to Table S1 indicates which molecular marker compounds were present in the quantification standards. The five dilutions were chosen to cover the range of concentrations anticipated in the atmosphere. After creating the dilutions, the quantification standards were spiked with the same internal standard mixture as the samples. Agilent Technology's MSD ChemStation software was used to quantify the peak areas of the molecular marker compounds and deuterated internal standard compounds in both the samples and the quantification standards. Each peak area was inspected and adjusted as necessary for quality control. Variable recovery in the extraction process and variable efficiency in the GC-MS analysis was accounted for by pairing the molecular marker compounds with internal standard compounds of similar structure and

working with the ratio of their peak areas. Table S1 in the supplemental material lists the internal standard paired with each molecular marker compound.

The GC-MS sequences were analyzed in larger batches covering between 4 and 13 sequences each, delineated by changes in GC-MS conditions (e.g., replacing the GC column or cleaning the MS source). Calibration curves were generated for each organic molecular species from all available runs of the quantification standards in a given batch to convert from peak area ratios to mass ratios observed at the five dilutions. A quadratic calibration curve fit to the quantification standard data was used with coefficients determined by weighted least squares. The weights were equal to the inverse variance in the peak area ratios at each of the five dilutions determined from the multiple runs of the quantification standards. This functional form adequately modeled the curvature present in the calibration points and down-weighted the effect of outlying calibration points. Figure S2 in the supplemental information contains several example calibration curves. The calibration curves generated for each batch along with the known mass of the internal standard compounds spiked onto the filters before extraction allowed for determination of the final mass amount (μg) of each molecular marker species present in the samples. For measurements below the range covered by the quantification standard dilutions, the calibration curve was extrapolated linearly through zero. For measurements above the range of the quantification standard dilutions, the calibration curve was extrapolated upward linearly by following the slope at the top end of the quadratic calibration curve. Any extrapolated values were flagged and used with caution.

Several compounds of interest were not present in the quantification standards and are identified as such in the footnote to Table S1 in the supplemental information. For these compounds, we used the calibration curve for the next closest compound present in the standards based on molecular structure and weight. In the case of two equal options (e.g., pentadecanoic acid which is halfway between tetradecanoic acid and hexadecanoic acid, both present in the quantification standards), a combined calibration curve was generated by including points from both neighboring compounds. This approach generated the best available unbiased amount estimates for these compounds. An example of a combined calibration curve is shown in Figure S2d in the supplemental information.

2.5 Uncertainty Estimation and Blank Correction

By incorporating multiple runs of the quantification standards at each dilution, we increased the precision of the organic molecular marker mass estimates and also provided a method for determining their uncertainty from the data. The residuals to the quadratic calibration curves were not normally distributed so parametric methods for determining the uncertainty estimates were not valid. Instead, the uncertainties in the peak area ratios were empirically derived from the calibration points at each dilution in the calibration curve using the following equation:

$$\delta PAR_k = \frac{1}{n_k - 1} \sum_{i=1}^{n_k} \left(PAR_i - PAR_{pred} \right)^2 \quad (1)$$

In Equation 1, δPAR_k is the empirically derived peak area ratio uncertainty measured at the kth dilution, n_k is the total number of calibration points included in the calibration curve at the kth dilution, PAR_i is the observed peak area ratio for the ith calibration point, and PAR_{pred} is the predicted peak area ratio based on the quadratic calibration curve. A piecewise polynomial was fit to these variances to allow for interpolation between the dilutions. The resulting empirical peak area ratio uncertainty (for a given mass ratio) was converted to a mass ratio uncertainty (for a given peak area) by multiplying by the slope of the inverted calibration curve at that point. This provided an estimated mass ratio uncertainty (standard deviation) as a

function of peak area ratio determined by the scatter in the calibration curve coming from multiple runs of the quantification standards in each batch. The functional form of Equation 1 was specifically chosen to give larger uncertainties to more variable calibration points. Figure S2 in the supplemental information shows the uncertainty bounds overlaid on the example calibration curves. This technique was only used for uncertainty estimation within the interpolation region of the calibration curve. For the region below the calibration curve, the absolute uncertainty was extrapolated down. For the region above the calibration curve, the relative uncertainty was extrapolated up. This gave conservative estimates for the uncertainty in the extrapolation region.

All molecular marker species were field blank corrected to account for background contamination. Outlier species in the field blanks were conservatively identified as any measurement greater than ten times the inner quartile range of all above detection limit field blank measurements for that species. The median value of the field blanks within a given batch (after outlier removal) was used to correct the observations in that batch. Many of the compounds had field blank levels not significantly different from zero. Nevertheless, for consistency across compounds and to incorporate noise present in the field blank measurements from each batch into the uncertainty estimates, field blank correction was performed on all species.

The root sum of squares (RSS) method (NIST, 1994) was used for uncertainty propagation to arrive at the final pointwise, blank corrected species concentration uncertainties. This involved combining the uncertainties estimated from the calibration curves discussed above with the uncertainty in the blank correction (estimated by the standard deviation of the field blank measurements in each batch) and the sample volume uncertainty. A detailed description of the application of the RSS method for uncertainty estimation in the bulk species along with the origin of the sample volume uncertainties is presented in Dutton et al. (2008). The pointwise uncertainty estimates for the organic molecular marker compounds complement estimates derived for the bulk species. They are advantageous to a single absolute or relative uncertainty applied across all measurements by allowing for changes in analysis conditions and batch-to-batch variability frequently encountered during long term studies.

3. RESULTS

3.1 Statistics and Temporal Variability

During the first year and a half of the DASH study (July 1, 2002 – December 31, 2003), 542 samples were collected, covering 99% of the available days in that period. Of these samples, 537 were analyzed for organic molecular markers by GC-MS (five samples between August 26 and September 1, 2002 were used for an alternate analysis). In addition, 77 weekly field blanks were collected and processed in parallel with the sample filters over the 1.5 years. The filters were analyzed in six separate batches ranging in size from 39 to 208 filters each. Eight weeks of samples (December 2, 2002 – January 26, 20003) were extracted and analyzed during a pilot phase to the DASH study and reanalyzed during the main analysis period along with the other filters. Considerable alkane contamination was present in the field blank extracts associated with the pilot analysis so the n-alkanes and cycloalkanes were all removed from the data set for this 8 week period. Other compound classes did not show disproportionate levels of contamination so they were left in the data set. Table 1 lists statistics for each individual organic molecular marker species including the number of valid samples, mean, coefficient of variation (CV = standard deviation/mean), median, maximum, mean value of the blank correction, mean uncertainty, signal to noise ratio (S/N = mean/mean uncertainty) and the percent of observations below detection limit (BDL). Table 2 contains statistics for daily meteorological measurements obtained during the study period from a nearby monitor located

in downtown Denver and operated by the Colorado Department of Public Health and Environment.

Figure 1 shows a time series of the markers summed by compound class. These plots reveal the high degree of day-to-day variability across all compound classes, particularly during the winter. The PAHs and methyl-PAHs, sterols and methoxyphenols have the most pronounced seasonality with higher values in the winter and lower values in the summer. Methoxyphenols are markers for biomass combustion; so too are many of the PAHs and sterols, but these compounds have important contributions from other sources as well. Methoxyphenols are therefore expected to be influenced by residential wood burning in the fall and winter and wildfires, prescribed burns and agricultural burning during the warmer seasons. The last week in November, 2002 has a pronounced increase in methoxyphenols (Figure 1g) and corresponding increase in the PAHs and methyl-PAHs (Figure 1b). One plausible explanation for this spike is increased residential wood burning and decreased atmospheric mixing during an early cold weather event surrounding the Thanksgiving holiday. The average ambient temperature during this period was 2 °C compared to 10 °C the week prior and 4 °C the week after. The highest methoxyphenol reading over the 1.5 years occurred on December 25, 2003 which could likewise be explained by increased residential wood burning during the Christmas holiday. Colorado had many wildfires in 2002 including the Hayman fire, the largest recorded wildfire in the state's history. This fire had significant impact on the air quality in Denver on two days in June, 2002 (Henderson et al., 2005;Vedal and Dutton, 2006). Unfortunately, our sample collection did not start until July, 2002 so we missed this event by a few weeks. None of the remaining wildfires in 2002 or any in 2003 were large enough or close enough to Denver to have direct impact on our receptor site and therefore the biomass combustion markers have little contribution to the overall organic carbon during the summer months.

The remaining classes of organic compounds in Figure 1 have significant contributions year round with a less pronounced drop in concentration during the summer. The alkanes and fatty acids show a short-duration summertime increase in June, July and August. This effect is amplified in the light odd n-alkanes (C23–C33) which is consistent with the odd/even alkane preferences found in source profiles for leaf abrasion (Cass, 1998;Rogge et al., 1993) and plant wax (Simoneit and Mazurek, 1982) suggesting a summertime biogenic source. All classes of compounds show a large number of high values in the late fall and winter resulting from frequent, short duration atmospheric inversions (Neff, 1997).

3.2 Temporal Correlations

Many of the molecular marker species demonstrated a high degree of correlation, especially within compound classes. Figures 2 – 5 contain correlation contour plots for each season which help illustrate the correlation structure among the molecular marker species. Also included in the plots are the bulk elemental carbon (EC) and organic carbon (OC) measurements discussed in Dutton et al. (2008). The six months of data from 2002 were excluded while generating this plot so that each season would receive equal representation using the complete year of 2003 data (winter = December 22 – March 21, spring = March 22 – June 20, summer = June 21 – September 20, fall = September 21 – December 21). Pearson's correlation coefficients (R) ranged from −0.37 (tridecanoic acid/methyl-228-PAH-sum) to 0.99 (octacosane/hexacosane) with correlations generally higher within compound classes. Several interesting patterns in the correlation contour plots are discussed in the upcoming Discussion section.

3.3 Relative Abundance and Seasonality of Compound Classes

As can be seen from the time series plots in Figure 1, there is strong seasonality to the molecular markers. This was also apparent in the time series for bulk species (Dutton et al., 2008). Figure 6 shows the relative contribution of the organic molecular markers by compound class annually

and during each of the four seasons defined above. Only the 2003 data was used for creating the stacked bars in Figure 6 to allow each season to have equal weight. The annual average of resolved organic molecular markers without derivatization was 67.7 ng/m^3 which represents roughly 1.5% of the organic mass presented in Dutton et al. (2008). Fatty acids were the most abundant of the molecular marker compound classes followed by alkanes and cycloalkanes. Methoxyphenols and PAHs showed the largest degree of seasonality, peaking in the fall and winter and reaching a minimum in the summer. A more detailed analysis of seasonal patterns will be the subject of a future paper.

4. DISCUSSION

4.1 Method Advancements

Time series health studies require continuous measurement of predictor variables to correlate with health outcomes over an extended period. Until recently, detailed organic measurements could not be used for such studies due to lengthy analysis times and prohibitively high detection limits. Reductions in analysis time were obtained for the current study by streamlining the organic extraction process, minimizing GC runtimes and using a high scan-rate MS system. Vast improvements in detection limits were obtained by practicing ultra-clean laboratory techniques and incorporating a high-volume injection PTV inlet, low-bleed column and inert ionization source in the GC-MS analysis. These improvements have provided the DASH study with a nearly complete daily speciated organics data set for source apportionment and health correlation analyses. The first 1.5 years of this data set have provided a unique look at the annual trends and correlation structure among numerous $PM_{2.5}$ molecular markers present in Denver.

4.2 Temporal Correlations

Source-specific organic molecular markers have demonstrated specificity and therefore are considered valuable for source apportionment work (Robinson et al., 2006b). Multivariate factor analysis methods in particular rely on temporal variability in the marker species to pull out common factors (Malinowski, 2002). Correlations between compounds, however, arise from more than just source commonality. Meteorology can cause species to vary together directly through dilution or indirectly through similar temperature driven processes. The correlation contour plots in Figures 2 – 5 illustrate the correlation structure present in the data set broken down by season and provide some insight into the relative roles of sources and meteorology.

The highest degree of correlation on average is found during the fall and winter when atmospheric inversions dictate the dilution conditions for all species. Despite the dominance of meteorology, within-class correlations stand out during the winter (Figure 2) and fall (Figure 5) for the light n-alkanes (tetracosane-triacontane), heavy n-alkanes (tritriacontane-tetracontane), steranes and methoxyphenols. There is also a high degree of correlation within the PAHs with the exception of fluoranthene, pyrene and retene. Fluoranthene and pyrene are the lightest two PAHs and are subject to volatilization during sampling and extraction; this is likely the reason for the poor correlation with the heavier, less volatile PAHs. Retene, which correlates with the methoxyphenols in most seasons better than the other PAHs, is emitted during combustion of resin acids found in conifer wood and is commonly considered a good source-specific marker for biomass combustion (Ramdahl, 1983;Schauer et al., 2001). It is, therefore, expected to be less well correlated with the other PAHs which may be coming from a combination of sources including motor vehicles, biomass combustion and industrial emissions.

During the spring and summer (Figures 3 and 4), the overall correlation goes down, but some very interesting source-driven correlations begin to stand out. The lighter n-alkanes (C22 – C32) and the heavier n-alkanoic acids (C14 – C18) reveal an odd/even correlation structure in the contour plot (depicted by the checkerboard patterns observed in the figures). This is consistent with the aliphatic odd/even carbon preferences (Hays et al., 2002; Schauer et al., 2001) found in source profiles for leaf abrasion (Cass, 1998; Rogge et al., 1993), plant waxes (Simoneit and Mazurek, 1982), combustion of certain wood species (Fine et al., 2002; Rogge et al., 1998) and cigarette smoke (Rogge et al., 1994). This pattern disappears in the higher weight n-alkanes (C33 – C40) which are above the range of alkanes measured in most source profile work. The steranes have strong correlations within class and with many of the PAHs and EC, indicative of a motor vehicle source. The methoxyphenols and retene continue to be well correlated, suggesting a common biomass combustion source. Finally, the oxy-PAHs appear to break into three groupings, the lighter oxy-PAHs (m/z = 168 – 180) which are not strongly correlated with any other class of compounds, the mid-weight oxy-PAHs (m/z = 196 – 208) which are correlated with the n-alkanoic acids, and the one heavy oxy-PAH (m/z = 230) which is correlated with most of the heavier PAHs. The origins of the oxy-PAHs are not currently known, but future source apportionment work may help to identify them.

4.3 Point Source Influences

Organic molecular markers have been used for numerous CMB source apportionment studies in the past (Fraser et al., 2003; Hannigan et al., 2005, Zheng et al., 2002). The source profiles used in CMB are primarily area sources such as motor vehicles, biomass combustion, food cooking, space heating and vegetative debris. Subramanian et al. (2007), however, found that local point sources in Pittsburgh, PA also frequently have a substantial contribution to the PAH concentrations and on a few days contribute significantly to the total organic aerosol. Specifically, emissions from local coke production were shown to be a dominant source of all PAHs on many days (Robinson et al., 2006b). Contributions from local point sources are likely to be influenced by meteorology (e.g., wind speed and direction) more so than area sources, and as a result their respective molecular markers should show a higher degree of day-to-day variability than markers for area sources.

Sheesley et al. (2007) compared the variability in select organic molecular markers to OC and EC by calculating the ratio of the maximum daily concentration to the annual average (max/mean ratio). They postulated that the max/mean ratios for OC and EC provide a rough estimate of the natural variability due to meteorology and anything greater than this might be due to the presence of local point sources contributing to the molecular markers. The max/mean ratio is highly susceptible to outliers in the data which may or may not be the result of point sources. Therefore, we chose instead to use the coefficient of variation (CV) in Table 1 as a more robust metric for comparing the relative variability of different species. The CV for mass, OC, EC, nitrate and sulfate during the first 1.5 years of the study was 0.6, 0.5, 0.7, 1.9 and 0.9, respectively. The CV for the molecular marker species varied from 0.4 – 2.0 for the PAHs, methyl-PAHs and oxy-PAHs, 0.6 – 0.8 for the steranes, 0.7 – 1.4 for the alkanes and cycloalkanes, 0.8 – 1.7 for the n-alkanoic acids and 1.3 – 2.1 for retene, stigmasterol and the methoxyphenols. This comparison suggests that most of the organic molecular markers have a similar degree of day-to-day variability compared to the bulk species. The higher values for retene and most of the methoxyphenols are on par with nitrate, all of which exhibit extreme seasonality that is inflating the CV. Limiting these molecular markers to winter reduces the range of CVs to 0.9 – 1.5, bringing them closer into line with the other species. When we compared the CVs measured in Denver to those measured in St. Louis and Pittsburgh, similar CVs were observed across sites for all species except 1) PAHs and oxy-PAHs which were higher in Pittsburgh relative to Denver and St. Louis and 2) oleic acid and cholesterol which were lower in Pittsburgh relative to Denver and St. Louis. We conclude, therefore, that the

majority of the organic molecular markers are not being influenced to a high degree by point sources in Denver.

Oleic acid and cholesterol are the two notable exceptions with CVs of 2.1 and 2.8, respectively. Since both these compounds are markers for meat cooking, it is plausible that our receptor site is being influenced by a local meat cooking source. The school cafeteria is located on the opposite end of the school, approximately 65 meters from our samplers. However, we did not see a significant weekday/weekend difference by season in either of these species which would be expected if the school cafeteria was the source. Survey results for day of the week barbeque use conducted by Chinkin et al. (2003) showed a two-fold increase in use on weekends. Again, the lack of a weekend difference in either species rules out nearby barbequing as a likely point source. Finally, there are no restaurants in the residential neighborhood surrounding our receptor site. It is therefore likely that frequent values below detection limit for oleic acid and cholesterol (69% and 73% of the time, respectively) are artificially driving up the CVs for these two relatively poorly quantified species.

4.4 Mobile Sources Influences

An elegant method for investigating the relative influence of similar sources on the molecular marker concentrations is the use of carefully selected ratio-ratio plots. Robinson et al. (2006a) developed this novel approach and have used it with varying success to isolate specific sources of cholestane emissions (Robinson et al., 2006a), PAH emissions (Robinson et al., 2006b), biomass combustion markers (Robinson et al., 2006c) and food cooking emissions (Robinson et al., 2006d). The basic principle is to generate plots comparing two species, each normalized by a third species. If there is only one source with consistent emission ratios for all three compounds and all three compounds are conserved in the atmosphere, then the ambient measurements should cluster around one point on the ratio-ratio plot corresponding to the emission characteristics of that source. If there are two sources with unique emission rates for the three compounds, the plot will reveal a continuum of points extending along a line between the locations of these two sources on the ratio-ratio plot. If there are three or more sources contributing to the three compounds, the ambient measurements should be constrained to a region defined by the location of the multiple sources on the ratio-ratio plot. Robinson et al. (2006a) presents several illustrative examples for each of these scenarios.

To explore evidence of a gasoline-diesel split present in our ambient data, we created two ratio-ratio plots containing different motor vehicle emission markers. The first of these plots is shown in Figure 7a and compares ba 30 norhopaneto ab hopane, both normalized by EC (hereafter referred to as the hopane ratio-ratio plot). The second is shown in Figure 7b and compares indeno[1,2,3-cd]pyrene to benzo[ghi]perylene, again normalized by EC (hereafter referred to as the PAH ratio-ratio plot. The ambient data in the plots are delineated by weekdays (Monday – Friday), weekends (Saturday and Sunday) and major holidays (New Years Day, Thanksgiving and Christmas). Overlaid on the plots are average source profiles from numerous vehicle emission studies as compiled by Robinson et al. (2006a,b) and average vehicle profiles specifically for Denver obtained during the Northern Front Range Air Quality Study (NFRAQS– Watson et al., 1998; Zielenska et al., 1998). The last heavy duty diesel profiles from NFRAQS (profile #9 in the figure) is not included in Figure 7b since indeno[1,2,3-cd] pyrene was reported as zero and therefore the ratio could not be included in the figure with logarithmic axes. A more recent motor vehicle emissions characterization study exists for the Southern California fleet (Fujita et al., 2007). These profiles were not included in Figure 7 but have the same general trend with the exception that the Southern California gasoline fleet has lower EC emissions than the profiles plotted so the gasoline vehicle profiles lie even further up to the right on the PAH ratio-ratio plot.

The ambient data lie nicely along a line in both ratio-ratio plots suggesting either a) a continuum of sources with emissions that lie along that line in the ratio-ratio plot or b) two dominant sources, one near each end of the ambient data resulting in a mixture of emissions falling along the line separating the two sources in the ratio-ratio plot. Based on the location of the emission source profiles, it would appear that the ambient hopane data in Figure 7a is best explained by a continuum of gasoline vehicle source compositions since the two NFRAQS heavy duty diesel source profiles deviate off the line explained by the data. The NFRAQS gasoline source profiles alone ranging from cleanest (low-emitter, profile #3) to dirtiest (smoker, profile #6) cover most of the range of the ambient measurements. Furthermore, there is no apparent difference between weekdays, weekends and holidays in the make-up of the ambient data which is consistent with a passenger vehicle dominated source.

In contrast, the ambient PAH data in Figure 7b is consistent with two dominant sources: gasoline vehicles in the upper right extreme and diesel vehicles in the lower left extreme. The day of the week delineation supports this interpretation since there are fewer weekend days clustered near the diesel vehicle source profiles, consistent with observations of reduced diesel truck traffic on weekends (Chinkin et al., 2004; Dreher and Harley, 1998; Harley et al., 2005; Motallebi et al., 2003). Furthermore, all of the holiday points fall within the range of the gasoline source profiles, consistent with a large and expected reduction in commerce-related diesel traffic on the major holidays.

The hopane ratio-ratio plot in Figure 7a can be directly compared to Figure 3 in Robinson et al. (2006a) for Pittsburgh, PA. The ambient data from both cities match up extremely well between the average gasoline and diesel profiles (profiles #1 and #2, respectively) reported in the Pittsburgh study. Since the NFRAQS light duty diesel profile (profile #7) also sits on this line, it is possible that a gasoline and light-duty diesel model would explain the Denver ambient data as well. However, the weekday/weekend and holiday observations continue to suggest that passenger vehicles are dominating these two hopane emissions.

Likewise, the PAH ratio-ratio plot in Figure 7b can be directly compared to Figure 4 in Robinson et al. (2006b) for Pittsburgh, PA. In this instance, the annual Pittsburgh data set is complicated by the evident contribution of a wood smoke source and a coke production source. The Denver data set, however, lies nicely on a continuum explained by the gasoline and diesel motor vehicle source profiles alone. This supports the conjecture that gasoline and diesel vehicles are the primary contributors to the selected PAHs and that these two sources have distinguishable emission ratios reflected in the ambient data.

4.5 Concluding Remarks

The daily speciated organics data presented in this paper have provided an unprecedented look at the chemical make-up and seasonal trends in numerous molecular marker compounds commonly used for source apportionment. Our results suggest that meteorology is the predominant factor controlling molecular marker concentrations; point sources do not appear to have a strong influence on our receptor site. In addition to the seasonal trends, many of the markers exhibit significant day-of-the-week trends which will be the subject of a future paper. The organic molecular marker data presented here is a subset of the final DASH data set which will cover five full years. The full data set will allow us to address the reproducibility of the seasonal trends and species correlations reported here. The full data set will also provide sufficient observations to perform source apportionment on a seasonal basis, thereby avoiding complications from seasonal variability in the molecular markers. Finally, the full data set will provide the necessary statistical for assessing associations with a variety of health endpoints, the primary aim of the DASH study.

Supplementary Material

Refer to Web version on PubMed Central for supplementary material.

Acknowledgments

This research is supported by NIEHS research grant number RO1 ES010197. Additional support for student assistance was provided by NSF Research Experience for Undergraduates award number EEC 0552895. We would like to extend a special thanks to Dr. Jamie Schauer and Dr. Alan Robinson for providing their results, thus making the comparisons between Denver, St. Louis and Pittsburgh possible. We would also like to thank Cathy Vos for her contribution to the organic extractions and Greg Brinkman for his programming expertise.

References

Bae MS, Schauer JJ, Turner JR. Estimation of the monthly average ratios of organic mass to organic carbon for fine particulate matter at an urban site. Aerosol Science and Technology 2006;40:1123–1139.

Cass GR. Organic molecular tracers for particulate air pollution sources. Trac-Trends in Analytical Chemistry 1998;17:356–366.

Cautreels W, Vancauwenberghe K. Determination of Organic-Compounds in Airborne Particulate Matter by Gas Chromatography Mass Spectrometry. Atmospheric Environment 1976;10:447–457.

Chinkin LR, Coe DL, Funk TH, Hafner HR, Roberts PT, Ryan PA, Lawson DR. Weekday versus weekend activity patterns for ozone precursor emissions in California's South Coast Air Basin. Journal of the Air & Waste Management Association 2003;53:829–843. [PubMed: 12880071]

Crimmins BS, Baker JE. Improved GC/MS methods for measuring hourly PAH and nitro-PAH concentrations in urban particulate matter. Atmospheric Environment 2006;40:6764–6779.

Dreher DB, Harley RA. A fuel-based inventory for heavy-duty diesel truck emissions. Journal of the Air & Waste Management Association 1998;48:352–358.

Dutton SJ, Schauer JJ, Vedal S, Hannigan MP. $PM_{2.5}$ characterization for time series studies: pointwise uncertainty estimation and bulk speciation methods applied in Denver. Atmospheric Environment. 2008 (submitted).

Fine PM, Cass GR, Simoneit BRT. Chemical characterization of fine particle emissions from the fireplace combustion of woods grown in the southern United States. Environmental Science & Technology 2002;36:1442–1451. [PubMed: 11999049]

Fraser MP, Yue ZW, Buzcu B. Source apportionment of fine particulate matter in Houston, TX, using organic molecular markers. Atmospheric Environment 2003;37:2117–2123.

Fujita EM, Zielinska B, Campbell DE, Arnott WP, Sagebiel JC, Mazzoleni L, Chow J, Gabele PA, Crews W, Snow R, Clark NN, Wayne WS, Lawson DR. Variations in speciated emissions from spark-ignition and compression-ignition motor vehicles in California's South Coast Air Basin. Journal of Air & Waste Management Association 2007;57:705–720.

Grahame TJ, Schlesinger RB. Health effects of airborne particulate matter: Do we know enough to consider regulating specific particle types or sources? Inhalation Toxicology 2007;19:457–481. [PubMed: 17497526]

Hannigan MP, Busby WF, Cass GR. Source contributions to the mutagenicity of urban particulate air pollution. Journal of the Air & Waste Management Association 2005;55:399–410. [PubMed: 15887882]

Harley RA, Marr LC, Lehner JK, Giddings SN. Changes in motor vehicle emissions on diurnal to decadal time scales and effects on atmospheric composition. Environmental Science & Technology 2005;39:5356–5362. [PubMed: 16082967]

Hays MD, Geron CD, Linna KJ, Smith ND, Schauer JJ. Speciation of gas-phase and fine particle emissions from burning of foliar fuels. Environmental Science & Technology 2002;36:2281–2295. [PubMed: 12075778]

HEI. Airborne particles and health: HEI epidemiologic evidence. Health Effects Institute Perspectives; Cambridge, MA: 2001. p. 1-8.

HEI. Understanding the health effects of components of the particulate matter mix: progress and next steps. Health Effects Institute Perspectives; Cambridge, MA: 2002. p. 1-20.

Henderson DE, Milford JB, Miller SL. Prescribed burns and wildfires in Colorado: Impacts of mitigation measures on indoor air particulate matter. Journal of the Air & Waste Management Association 2005;55:1516–1526. [PubMed: 16295277]

Jaeckels JM, Bae MS, Schauer JJ. Positive matrix factorization (PMF) analysis of molecular marker measurements to quantify the sources of organic aerosols. Environmental Science & Technology 2007;41:5763–5769. [PubMed: 17874784]

Lippmann M, Frampton M, Schwartz J, Dockery D, Schlesinger R, Koutrakis P, Froines J, Nel A, Finkelstein J, Godleski J, Kaufman J, Koenig J, Larson T, Luchtel D, Liu LJS, Oberdorster G, Peters A, Sarnat J, Sioutas C, Suh H, Sullivan J, Utell M, Wichmann E, Zelikoff J. The US Environmental Protection Agency particulate matter health effects research centers program: A midcourse report of status, progress, and plans. Environmental Health Perspectives 2003;111:1074–1092. [PubMed: 12826479]

Malinowski, ER. Factor analysis in chemistry. Wiley; New York: 2002.

Mazurek MA, Simoneit BRT, Cass GR, Gray HA. Quantitative High-Resolution Gas-Chromatography and High-Resolution Gas-Chromatography Mass-Spectrometry Analyses of Carbonaceous Fine Aerosol-Particles. International Journal of Environmental Analytical Chemistry 1987;29:119–139.

Motallebi N, Tran H, Croes BE, Larsen LC. Day-of-week patterns of particulate matter and its chemical components at selected sites in California. Journal of the Air & Waste Management Association 2003;53:876–888. [PubMed: 12880074]

Neff WD. The Denver Brown Cloud studies from the perspective of model assessment needs and the role of meteorology. Journal of the Air & Waste Management Association 1997;47:269–285.

NIST. Technical note 1297, 1994 edition: Guidelines for evaluating and expressing the uncertainty of NIST measurement results. National Institute of Standards and Technology; 1994. http://physics.nist.gov/Pubs/guidelines/appa.html

Pang Y, Turpin BJ, Gundel LA. On the importance of organic oxygen for understanding organic aerosol particles. Aerosol Science and Technology 2006;40:128–133.

Pio C, Alves C, Duarte A. Organic components of aerosols in a forested area of central Greece. Atmospheric Environment 2001;35:389–401.

Ramdahl T. Retene - a Molecular Marker of Wood Combustion in Ambient Air. Nature 1983;306:580–583.

Robinson AL, Donahue NM, Rogge WF. Photochemical oxidation and changes in molecular composition of organic aerosol in the regional context. Journal of Geophysical Research-Atmospheres 2006a; 111:1–15.

Robinson AL, Subramanian R, Donahue NM, Bernardo-Bricker A, Rogge WF. Source apportionment of molecular markers and organic aerosols-1. Polycyclic aromatic hydrocarbons and methodology for data visualization. Environmental Science & Technology 2006b;40:7803–7810. [PubMed: 17256531]

Robinson AL, Subramanian R, Donahue NM, Bernardo-Bricker A, Rogge WF. Source apportionment of molecular markers and organic aerosol. 2. Biomass smoke. Environmental Science & Technology 2006c;40:7811–7819. [PubMed: 17256532]

Robinson AL, Subramanian R, Donahue NM, Bernardo-Bricker A, Rogge WF. Source apportionment of molecular markers and organic aerosol. 3. Food cooking emissions. Environmental Science & Technology 2006d;40:7820–7827. [PubMed: 17256533]

Rogge WF, Hildemann LM, Mazurek MA, Cass GR. Sources of fine organic aerosol. 6. cigarette-smoke in the urban atmosphere. Environmental Science & Technology 1994;28:1375–1388.

Rogge WF, Hildemann LM, Mazurek MA, Cass GR, Simoneit BRT. Sources of fine organic aerosol. 4. particulate abrasion products from leaf surfaces of urban plants. Environmental Science & Technology 1993;27:2700–2711.

Rogge WF, Hildemann LM, Mazurek MA, Cass GR, Simoneit BRT. Sources of fine organic aerosol. 9. pine, oak and synthetic log combustion in residential fireplaces. Environmental Science & Technology 1998;32:13–22.

Rogge WF, Hildemann LM, Mazurek MA, Cass GR, Simonelt BRT. Sources of fine organic aerosol. 1. charbroilers and meat cooking operations. Environmental Science & Technology 1991;25:1112–1125.

Schauer JJ, Kleeman MJ, Cass GR, Simoneit BRT. Measurement of emissions from air pollution sources. 2. C-1 through C-30 organic compounds from medium duty diesel trucks. Environmental Science & Technology 1999;33:1578–1587.

Schauer JJ, Kleeman MJ, Cass GR, Simoneit BRT. Measurement of emissions from air pollution sources. 3. C-1-C-29 organic compounds from fireplace combustion of wood. Environmental Science & Technology 2001;35:1716–1728. [PubMed: 11355184]

Schauer JJ, Rogge WF, Hildemann LM, Mazurek MA, Cass GR. Source apportionment of airborne particulate matter using organic compounds as tracers. Atmospheric Environment 1996;30:3837–3855.

Schwarze PE, Ovrevik J, Lag M, Refsnes M, Nafstad P, Hetland RB, Dybing E. Particulate matter properties and health effects: consistency of epidemiological and toxicological studies. Human & Experimental Toxicology 2006;25:559–579. [PubMed: 17165623]

Sheesley RJ, Schauer JJ, Meiritz M, DeMinter JT, Bae MS, Turner JR. Daily variation in particle-phase source tracers in an urban atmosphere. Aerosol Science and Technology 2007;41:981–993.

Simoneit BRT, Mazurek MA. Organic-Matter of the Troposphere .2. Natural Background of Biogenic Lipid Matter in Aerosols over the Rural Western United-States. Atmospheric Environment 1982;16:2139–2159.

Subramanian R, Donahue NM, Bernardo-Bricker A, Rogge WF, Robinson AL. Insights into the primary-secondary and regional-local contributions to organic aerosol and $PM_{2.5}$ mass in Pittsburgh, Pennsylvania. Atmospheric Environment 2007;41:7414–7433.

Turpin BJ, Lim HJ. Species contributions to $PM_{2.5}$ mass concentrations: Revisiting common assumptions for estimating organic mass. Aerosol Science and Technology 2001;35:602–610.

Vedal S, Dutton SJ. Wildfire air pollution and daily mortality in a large urban area. Environmental Research 2006;102:29–35. [PubMed: 16716288]

Vedal S, Hannigan MP, Dutton SJ, Miller SL, Milford JB, Rabinovitch N, Kim SY, Sheppard L. The Denver Aerosol Sources and Health (DASH) study: overview and early findings. Atmospheric Environment. 2008 (submitted).

Watson, JG.; Fujita, E.; Chow, J.; Zielinska, B.; Richards, LW.; Neff, W.; Dietrich, D. Northern Front Range Air Quality Study final report. Desert Research Institute; Reno, NV: 1998. Prepared for Colorado State University, Fort Collins, CO and Electric Power Research Institute, Palo Alto, CA. DRI Document No. 6580-685-8750-2F2

White WH, Roberts PT. On the nature and origins of visibility-reducing aerosols in the Los Angeles air basin. Atmospheric Environment 1977;11:803–812.

Wittig AE, Anderson N, Khlystov AY, Pandis SN, Davidson C, Robinson AL. Pittsburgh air quality study overview. Atmospheric Environment 2004;38:3107–3125.

Wylie, PL. Trace level pesticide analysis by GC/MS using large-volume injection. Agilent Technologies, Inc.; Wilmington, DE: 1997. p. 1-10.

Zheng M, Cass GR, Schauer JJ, Edgerton ES. Source apportionment of $PM_{2.5}$ in the southeastern United States using solvent-extractable organic compounds as tracers. Environmental Science & Technology 2002;36:2361–2371. [PubMed: 12075791]

Zielinska, B.; McDonald, J.; Hayes, T.; Chow, JC.; Fujita, EM.; Watson, JG. Northern Front Range Air Quality Study final report, volume b: source measurements. Desert Research Institute; Reno, NV: 1998. Prepared for Colorado State University, Fort Collins, CO

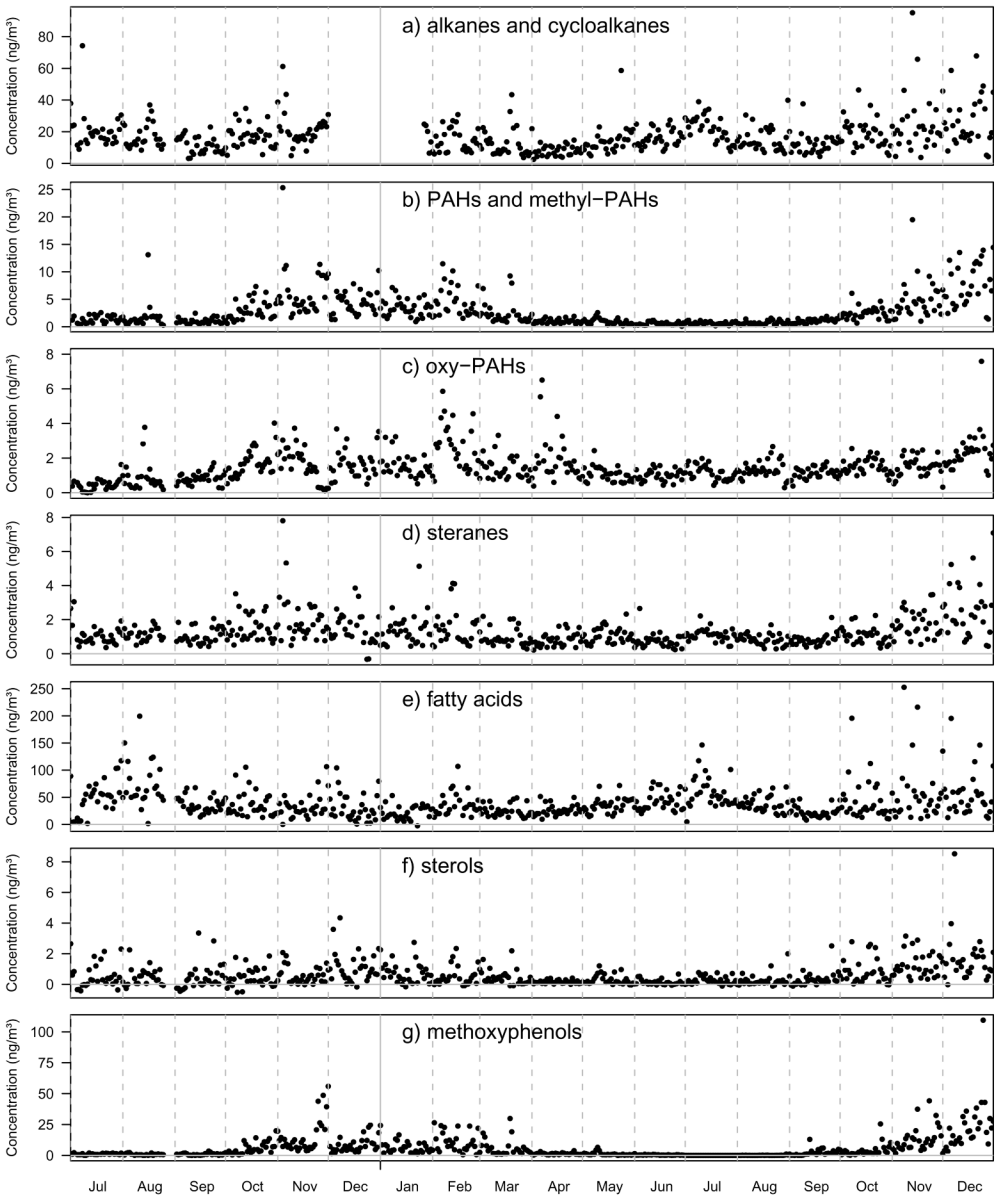

Figure 1.

Time series plots of $PM_{2.5}$ organic molecular marker compounds from July 1, 2002 through December 31, 2003 summed by compound class.

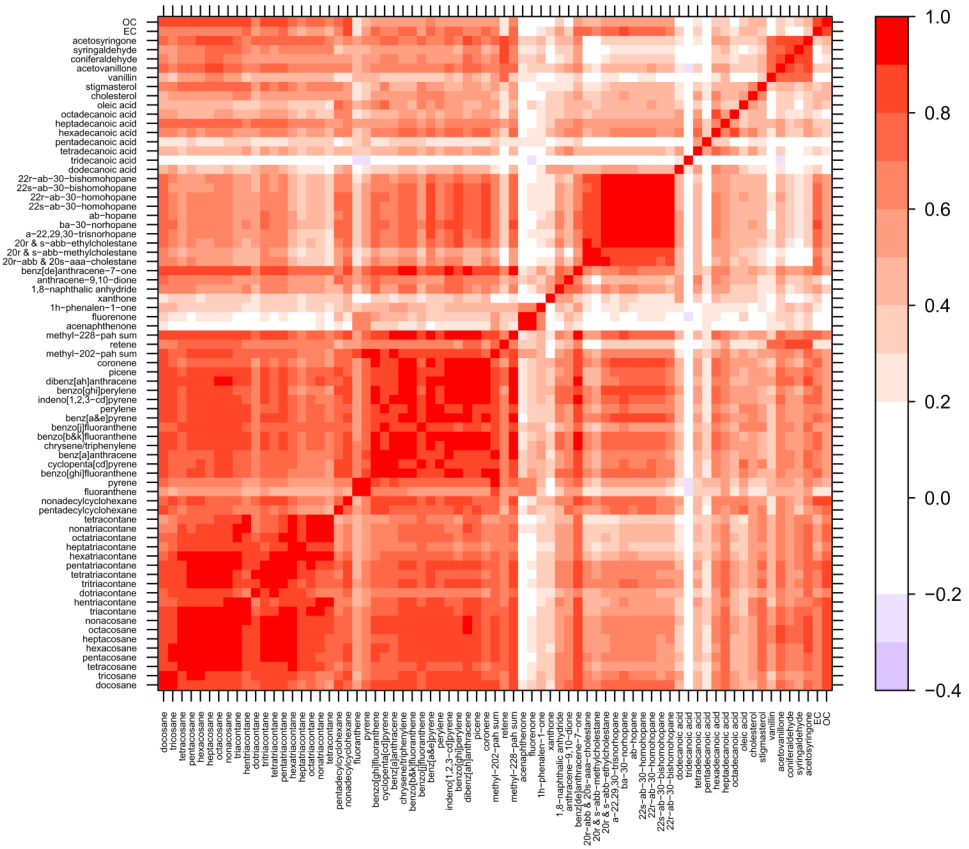

Figure 2.

Winter 2003 (January 1 – March 21 and December 22 – December 31) correlation contour plots illustrating the Pearson's correlation coefficient (R) between the 71 different organic molecular markers and the bulk carbon measurements. Compounds are grouped by compound class and sorted by increasing molecular weight within each class.

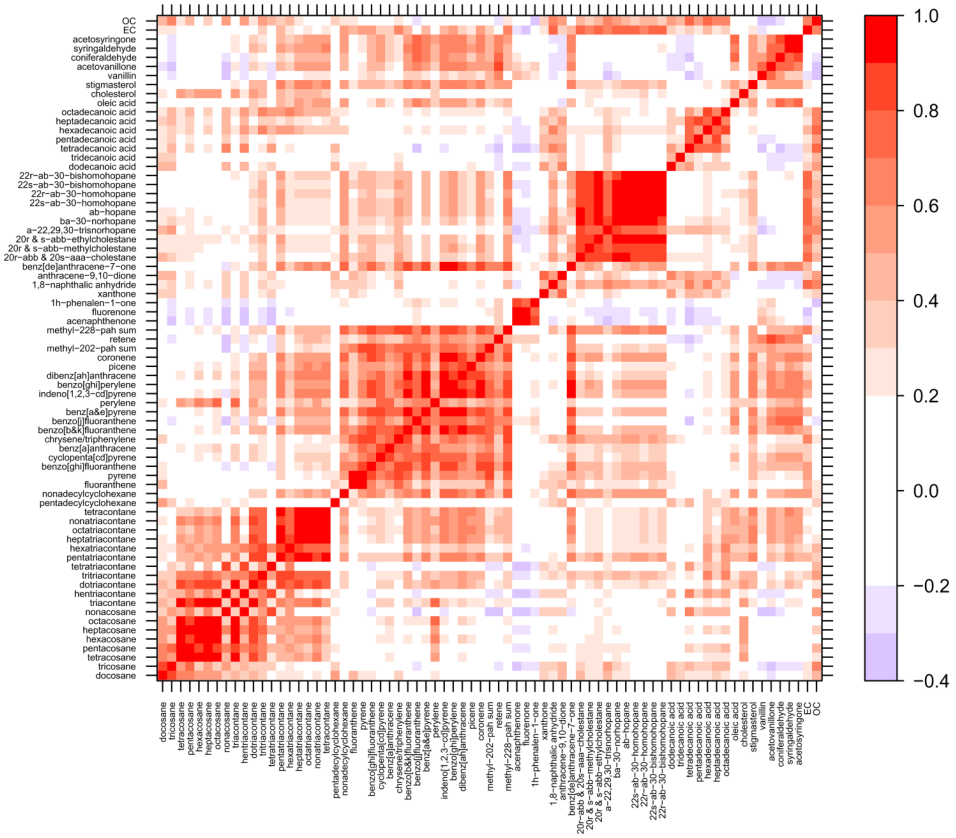

Figure 3.

Spring 2003 (March 22 – June 20) correlation contour plots illustrating the Pearson's correlation coefficient (R) between the 71 different organic molecular markers and the bulk carbon measurements. Compounds are grouped by compound class and sorted by increasing molecular weight within each class.

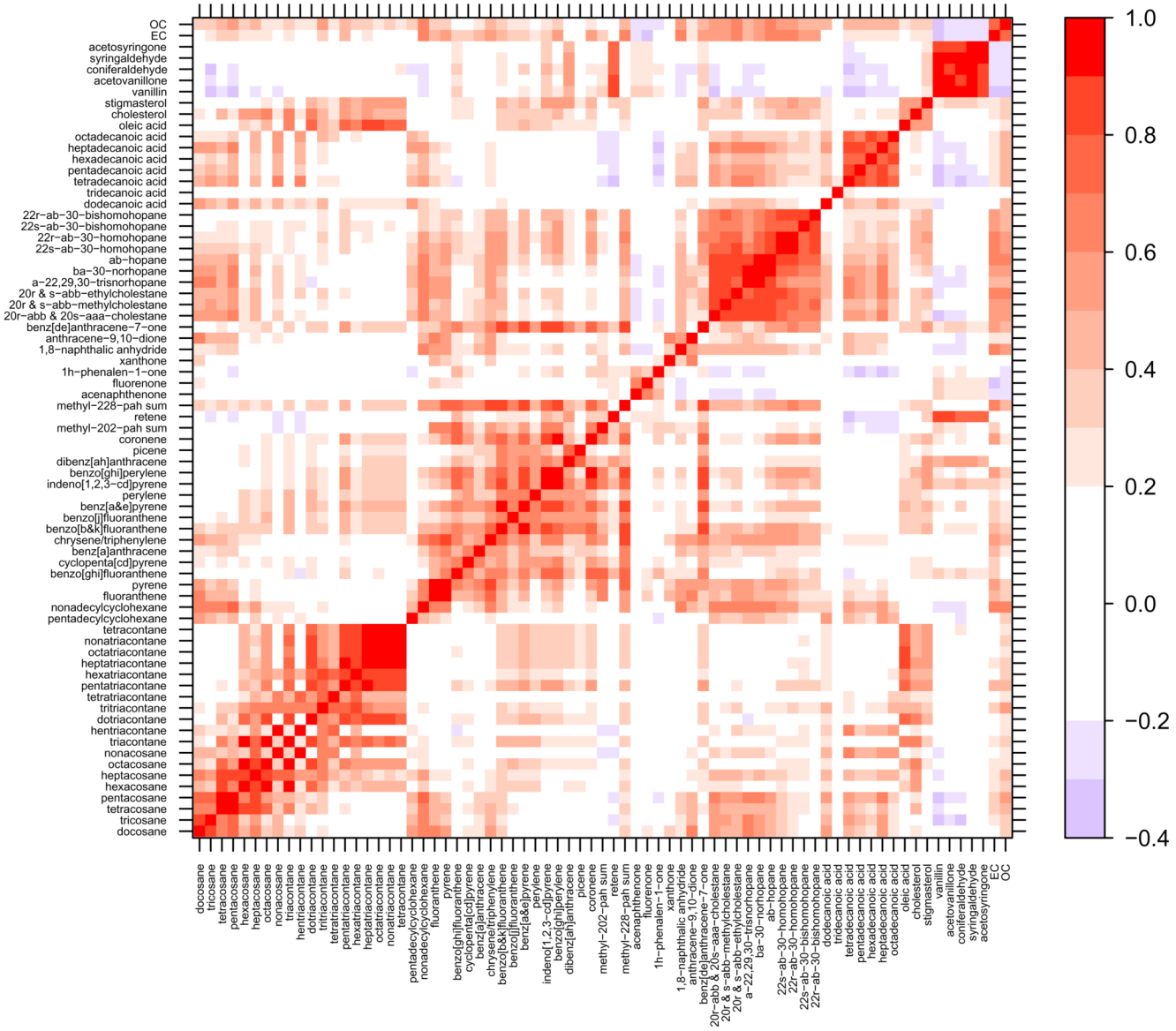

Figure 4.

Summer 2003 (June 21 – September 20) correlation contour plots illustrating the Pearson's correlation coefficient (R) between the 71 different organic molecular markers and the bulk carbon measurements. Compounds are grouped by compound class and sorted by increasing molecular weight within each class.

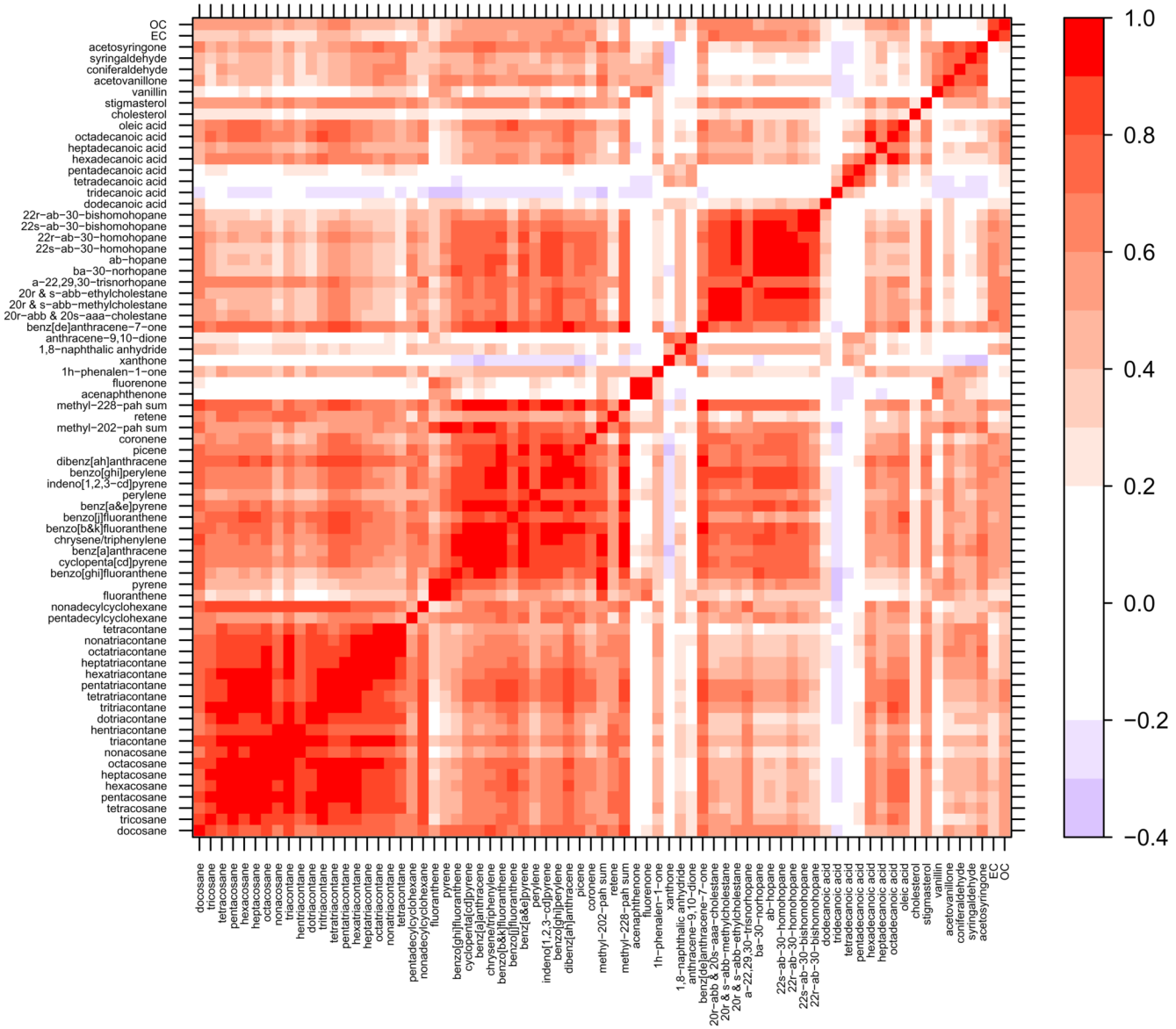

Figure 5.

Fall 2003 (September 21 – December 21) correlation contour plots illustrating the Pearson's correlation coefficient (R) between the 71 different organic molecular markers and the bulk carbon measurements. Compounds are grouped by compound class and sorted by increasing molecular weight within each class.

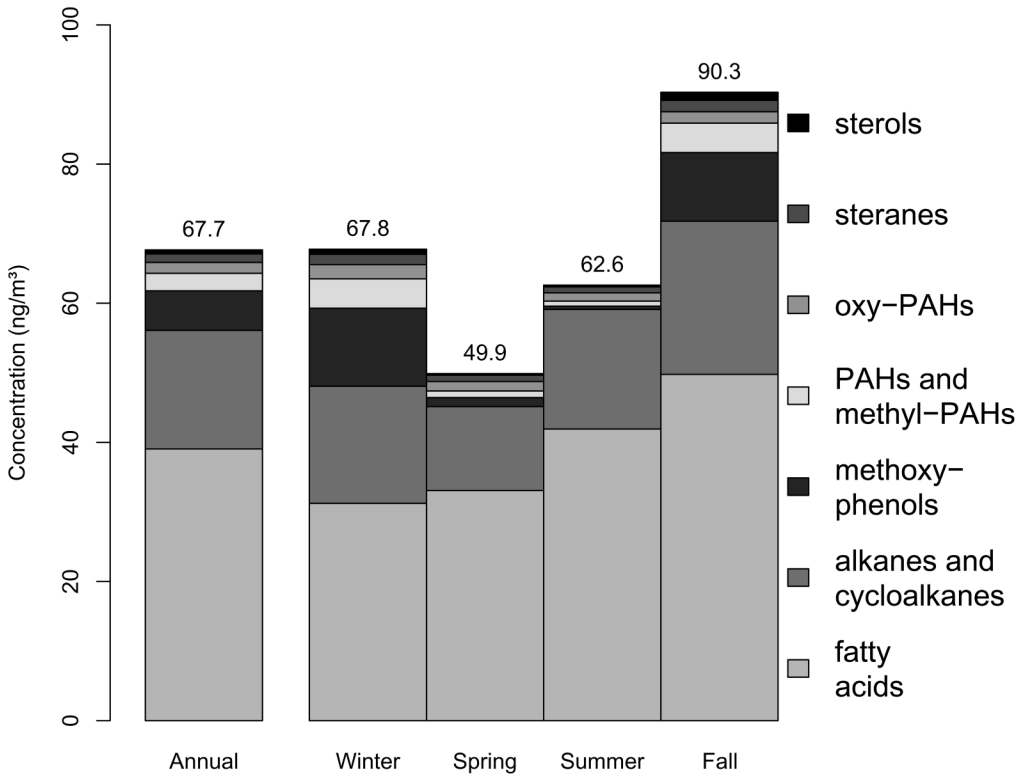

Figure 6.
Resolved organic molecular markers broken down by compound class and season. The sum of all species averaged annually and by season is displayed above the corresponding bars.

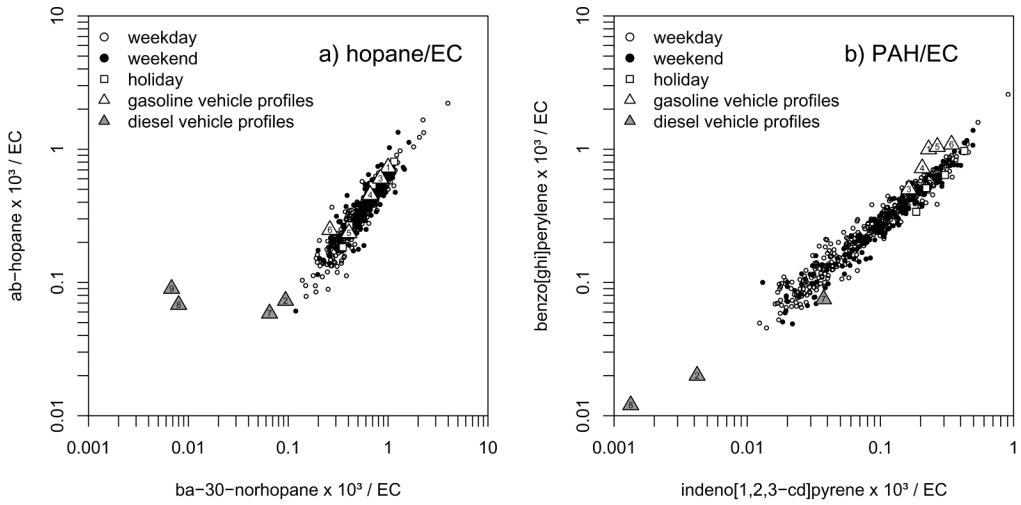

Figure 7.

Ratio-ratio plots for a) two hopanes normalized by EC and b) two polycyclic aromatic hydrocarbons (PAHs) normalized by EC covering 1.5 years of daily measurements. The ambient measurements are stratified by weekdays, weekends and holidays (New Years, Thanksgiving and Christmas). The numbered triangles represent the location of published gasoline and diesel vehicle emission profiles on the ratio-ratio plots. Profiles 1 and 2 are from Robinson et al. (2006a,b) and represent an average of many published mobile source profiles for 1) gasoline vehicles and 2) diesel vehicles. Profiles 3 – 8 are from the NFRAQS study (Zielenska et al., 1998) and represent average Denver mobile source profiles for 3) low emitter gasoline vehicles, 4) non-smoking gasoline vehicles, 5) high emitter gasoline vehicles, 6) smoking gasoline vehicles, 7) light duty diesel vehicles and 8) heavy duty diesel vehicles. Profile 9 is from a separate published report on the NFRAQS study (Watson et al., 1998) for 9) heavy duty diesel vehicles.

Table 1

Statistics for each molecular marker species based on 1.5 years of data (July 1, 2002 to December 31, 2003).

Chemical Species	Number of Days	Mean (ng/m^3)	CV ( )[a]	Median (ng/m^3)	Max (ng/m^3)	Mean Blank Corr. (ng/m^3) [b]	Mean Unc (ng/m^3)[c]	S/N ( )[d]	BDL (%)[e]
alkanes and cycloalkanes									
docosane	479	1.45	0.67	1.20	7.74	0.04	0.11	13.4	0%
tricosane	479	2.16	0.75	1.70	10.94	0.04	0.21	10.5	0%
tetracosane	478	1.13	0.68	0.96	6.00	0.06	0.16	7.0	1%
pentacosane	479	1.65	0.68	1.37	9.03	0.07	0.19	8.7	1%
hexacosane	479	0.92	0.84	0.66	5.97	0.07	0.13	6.9	8%
heptacosane	479	1.29	0.70	1.08	7.94	0.07	0.15	8.5	5%
octacosane	479	0.86	0.96	0.57	6.50	0.08	0.14	6.2	17%
nonacosane	479	1.91	0.75	1.57	11.19	0.06	0.20	9.7	3%
triacontane	479	0.70	1.07	0.43	5.96	0.05	0.12	5.7	19%
hentriacontane	479	1.75	0.85	1.40	11.73	0.05	0.25	6.9	1%
dotriacontane	477	0.47	1.36	0.25	5.68	0.03	0.17	2.7	49%
tritriacontane	479	0.79	0.81	0.63	5.13	0.02	0.09	8.4	3%
tetratriacontane	479	0.58	0.93	0.43	3.64	0.02	0.07	8.1	9%
pentatriacontane	479	0.45	0.92	0.33	2.72	0.01	0.06	7.7	8%
hexatriacontane	479	0.26	1.06	0.16	1.85	0.01	0.05	5.7	22%
heptatriacontane	479	0.19	1.22	0.10	1.70	0.01	0.04	4.9	35%
octatriacontane	479	0.15	1.25	0.08	1.30	0.01	0.04	3.8	49%
nonatriacontane	479	0.15	1.14	0.09	1.15	0.01	0.04	3.8	51%
tetracontane	440	0.10	1.29	0.05	1.03	0.00	0.04	2.9	59%
pentadecylcyclohexane	470	0.16	1.24	0.11	1.90	0.00	0.02	9.0	8%
nonadecylcyclohexane	479	0.15	0.87	0.11	1.33	0.00	0.02	7.6	7%
PAHs									
fluoranthene	536	0.19	0.92	0.13	1.15	0.01	0.03	6.3	4%
pyrene	536	0.16	1.12	0.09	1.41	0.01	0.02	8.1	3%
benzo[ghi]fluoranthene	536	0.10	1.06	0.06	1.00	0.00	0.01	14.5	0%
cyclopenta[cd]pyrene	536	0.04	1.45	0.02	0.41	0.00	0.00	10.9	5%
benz[a]anthracene	536	0.06	1.21	0.03	0.38	0.00	0.01	10.9	3%

Chemical Species	Number of Days	Mean (ng/m^3)	CV ( )[a]	Median (ng/m^3)	Max (ng/m^3)	Mean Blank Corr. (ng/m^3) [b]	Mean Unc (ng/m^3)[c]	S/N ( )[d]	BDL (%)[e]
chrysene/triphenylene	536	0.17	0.93	0.12	2.01	0.00	0.02	10.9	0%
benzo[b&k]fluoranthene	536	0.22	1.12	0.14	3.00	0.00	0.02	9.0	0%
benzo[j]fluoranthene	536	0.01	1.99	0.00	0.16	0.00	0.00	3.0	60%
benz[a&e]pyrene	536	0.18	1.35	0.10	3.27	0.00	0.02	9.2	4%
perylene	536	0.01	1.88	0.00	0.23	0.00	0.00	3.0	60%
indeno[1,2,3-cd]pyrene	536	0.08	1.05	0.05	0.59	0.00	0.01	8.8	6%
benzo[ghi]perylene	536	0.21	1.04	0.13	1.69	0.00	0.02	9.7	4%
dibenz[ah]anthracene	536	0.02	1.37	0.01	0.17	0.00	0.00	4.9	44%
picene	536	0.01	1.46	0.01	0.14	0.00	0.00	4.7	44%
coronene	536	0.10	1.01	0.07	0.93	0.00	0.01	7.2	8%
methyl-202-PAH sum	536	0.62	1.13	0.35	6.66	0.02	0.08	7.7	2%
retene	536	0.42	2.07	0.16	11.06	0.01	0.06	6.7	23%
methyl-228-PAH sum	535	0.11	0.91	0.08	1.01	0.00	0.01	7.9	1%
oxy-PAHs									
acenaphthenone	529	0.10	1.69	0.03	1.47	0.01	0.02	5.0	49%
fluorenone	529	0.36	1.26	0.21	3.43	0.02	0.06	6.1	26%
1H-phenalen-1-one	529	0.25	1.12	0.19	3.68	0.00	0.03	7.2	5%
xanthone	462	0.15	0.67	0.14	0.56	0.00	0.02	8.7	10%
1,8-naphthalic anhydride	462	0.31	0.59	0.27	1.56	0.00	0.04	8.4	0%
anthracene-9,10-dione	462	0.32	0.44	0.30	0.90	0.00	0.04	8.4	1%
benz[de]anthracene-7-one	536	0.08	0.96	0.05	0.68	0.00	0.01	11.3	2%
steranes									
20R-abb & 20S-aaa-cholestane	535	0.14	0.62	0.12	0.71	0.00	0.01	9.7	2%
20R & S-abb-methylcholestane	535	0.10	0.81	0.08	0.77	0.00	0.01	9.4	4%
20R & S-abb-ethylcholestane	535	0.11	0.64	0.09	0.52	0.00	0.01	9.1	3%
a-22,29,30-trisnorhopane	535	0.09	0.64	0.08	0.43	0.00	0.01	9.2	3%
ba-30-norhopane	535	0.35	0.77	0.27	2.52	0.01	0.03	12.0	0%
ab-hopane	535	0.22	0.78	0.17	1.67	0.01	0.03	7.3	2%
22S-ab-30-homohopane	535	0.10	0.83	0.07	0.74	0.00	0.01	7.3	3%
22R-ab-30-homohopane	534	0.07	0.84	0.05	0.49	0.00	0.01	6.8	4%
22S-ab-30-bishomohopane	535	0.06	0.82	0.05	0.41	0.00	0.01	6.5	5%

Chemical Species	Number of Days	Mean (ng/m^3)	CV ( )[a]	Median (ng/m^3)	Max (ng/m^3)	Mean Blank Corr. (ng/m^3) [b]	Mean Unc (ng/m^3)[c]	S/N ( )[d]	BDL (%)[e]
22R-ab-30-bishomohopane	535	0.05	0.81	0.04	0.33	0.00	0.01	6.1	7%
fatty acids									
dodecanoic acid	521	3.08	0.80	2.38	18.86	0.16	0.44	7.0	5%
tridecanoic acid	520	0.22	1.66	0.00	2.73	0.00	0.15	1.5	79%
tetradecanoic acid	526	4.58	0.99	2.92	33.10	0.13	0.66	6.9	4%
pentadecanoic acid	526	0.99	0.97	0.75	9.60	0.01	0.18	5.4	11%
hexadecanoic acid	526	18.08	0.75	14.53	107.00	2.18	3.28	5.5	6%
heptadecanoic acid	526	0.62	0.98	0.46	4.03	0.00	0.27	2.3	38%
octadecanoic acid	526	11.28	0.96	8.63	117.63	2.32	3.37	3.3	16%
oleic acid	525	2.04	2.83	0.00	56.45	0.03	0.40	5.1	69%
sterols and methoxyphenols									
cholesterol	535	0.24	2.14	0.12	8.21	0.21	0.21	1.1	73%
stigmasterol	535	0.35	1.33	0.17	4.04	0.00	0.07	5.2	29%
vanillin	535	2.44	1.84	0.97	67.40	0.06	0.38	6.4	21%
acetovanillone	533	0.58	1.45	0.24	5.63	0.00	0.08	7.0	34%
coniferaldehyde	536	1.21	1.75	0.35	13.66	0.00	0.17	7.1	37%
syringaldehyde	521	1.20	1.82	0.19	17.86	0.00	0.16	7.5	47%
acetosyringone	536	0.29	2.09	0.02	5.64	0.00	0.05	5.6	56%

[a] Coefficient of variation (CV) = standard deviation/mean

[b] Mean value of the field blank corrections expressed as a concentration.

[c] Mean value of the propagated concentration uncertainty.

[d] Signal to noise ratio (mean concentration/mean uncertainty).

[e] Percent of observations not significantly different from zero using a 95% confidence interval.

Table 2

Meteorological statistics based on 1.5 years of hourly observations in downtown Denver (July 1, 2002 to December 31, 2003).

Parameter	Statistic	Annual	Winter	Spring	Summer	Fall
temperature (°C)	mean	13	4	14	24	8
	SD[a]	10	6	6	4	7
	mean daily max[b]	20	10	21	31	15
	mean daily min[c]	7	−2	8	17	2
relative humidity (%)	mean	45	48	49	39	47
	SD[a]	17	20	16	13	18
	mean daily max[b]	67	68	74	63	68
	mean daily min[c]	26	29	27	21	28
scalar wind speed ($km\ h^{-1}$)	mean	8	8	9	8	8
	SD[a]	2	2	2	1	2
	mean daily maxe[b]	15ee	16	17	15	14
	mean daily min[c]	4	4	4	3	4

[a] Standard deviation (SD) of the daily means.

[b] Mean of the daily maximum observation.

[c] Mean of the daily minimum observation.